

VIBRATION ANALYSIS OF A HALF-CAR MODEL WITH SEMI-ACTIVE DAMPING

URSZULA FERDEK, JAN ŁUCZKO

Cracow University of Technology, Faculty of Mechanical Engineering, Krakow, Poland

e-mail: uferdek@mech.pk.edu.pl; jluczko@mech.pk.edu.pl

In this paper, analysis of a half-car model with linear and nonlinear semi-active dampers is performed. Using Matlab-Simulink software, a response of the system to a harmonic excitation of variable frequency and to an impulse excitation is found. The effect of both the distribution of spring-supported mass and the asymmetry of the support on the frequency characteristics of velocities and displacements at the mounting points of the dampers are analyzed. Additionally, characteristics of forces generated by the semi-active dampers and the response of the system when crossing an obstacle are determined.

Keywords: semi-active damper, vibration damping, car suspension, hysteresis

Notations

a_0	– excitation amplitude
c_b	– sum of damping parameters of suspension
$c_{1f}, c_{2f}, c_{1r}, c_{2r}$	– damping parameters of front and rear semi-active damper
c_{wf}, c_{wr}	– damping coefficients of front and rear wheel
I_b	– moment of inertia of body
k_{bf}, k_{br}, k_b	– stiffness of front and rear spring, sum of stiffness
k_{wf}, k_{wr}	– stiffness parameters of front and rear wheel
l_f, l_r	– distance of axles from center of body mass
l	– distance between both axles
m_b, m_{wf}, m_{wr}	– mass of body (spring-supported mass), front and rear wheel (non-spring-supported mass)
$p^{min}, p^{max}, p^{mean}$	– minimum, maximum and the mean value of the parameter p
t_0	– delay time of kinematic excitation acting on rear wheel
u_f, u_r	– control force of front and rear semi-active dampers
V_0	– driving speed
v_{bf}, v_{br}	– dimensionless velocity of front and rear body points
w_f, w_r	– kinematic excitation applied to front and rear wheel
$x_{bf}, x_{br}, x_{wf}, x_{wr}$	– dimensionless displacements of body points, front and rear wheel
y_b	– displacement of center of body mass
$y_{bf}, y_{br}, y_{wf}, y_{wr}$	– displacements of body points and front and rear wheel
α, α_0	– dimensionless and dimensional scaling factors of Bouc-Wen force
β, γ, A, n	– control shape parameters of hysteresis loops
δ	– dimensionless amplitude of parameters $c_{1f}, c_{2f}, c_{1r}, c_{2r}, \alpha_{0f}, \alpha_{0r}$
κ_c	– ratio of stiffness of front spring to sum of stiffnesses
η	– dimensionless excitation frequency
λ	– mass distribution index of body

ϕ_b	–	angle of rotation of body
ω, ω_0	–	excitation and reference frequency

1. Introduction

The primary cause of vibrations affecting the driver of a car are kinematic disturbances resulting from road surface irregularities. Elimination of these vibrations is essential in order to improve both the comfort and the safety of the passenger. When the vehicle is driving across a road with large irregularities (obstacles), its wheels might get separated from the surface of the road, which in turn decreases the efficiency of force transmission of the drive, braking and steering systems of the car. An improved driving dynamics and better road traction on curves and bumps can be achieved by using the so-called “hard suspension”. However, the cost is the reduction of comfort of the passenger. The criteria for assessing the quality of shock absorbers should therefore include both the minimization of car body vibration and appropriate wheel-road adhesion (Łuczko and Ferdek, 2012).

In order to perform dynamical analysis, either a quarter-car (Gopala Rao and Narayanan, 2009; Huang and Chen, 2006) or a half-car (Ihsan *et al.*, 2009; Sapiński and Rosół, 2008) model can be used. The quarter-car model that consists of a non spring-supported mass (a wheel with partial of suspension) and a spring-supported mass (1/4 car body) is a two-degrees of freedom model and is usually used for testing of the performance of control algorithms. The half-car four-degrees of freedom model consist of two non-spring supported masses and a spring-supported one (1/2 car body). It additionally includes rotation angle of the body and allows analysis of the response to the excitation applied to both wheels of the vehicle.

Dampers used in the suspension system can be either passive, semi-active or active. Dynamical properties of the dampers are usually defined by models with hysteresis characteristics, such as Bingham (Prabakar *et al.*, 2009), Bouc-Wen (Dominguez *et al.*, 2008; Yao *et al.*, 2002) or Spencer model (Spencer *et al.*, 1996).

Requirements set for the comfort and safety of driving can be fulfilled by using semi-active suspension systems, introduced by Crosby and Karnopp (1973). In comparison to passive ones, the semi-active systems allow the damping force to be adjusted depending on driving conditions. Additionally, they require less power than similar active systems.

Several methods of control have been used, some of which can be found in the paper by Ahmadian (2001). Liu *et al.* (2005) as well as Wu and Griffin (1997), when analyzing on-off control, assume that the damping force should be high if the product of relative and absolute velocity is more than zero. Fischer and Isermann (2004) analyzed the relation between parameters of the car suspension system and the driving comfort as well as the safety indexes. They defined the comfort index as the effective acceleration value while the safety index as the effective ratio of the dynamic and static response. In the study by Sapiński and Martynowicz (2005), the results were presented for the theoretical and experimental half-car model, in which the car suspension was controlled by two separate magneto-rheological dampers (MR damper).

Some interesting options for control of a semi-active car suspension were presented by Ahmadian (2001). The most common model to be analyzed was the quarter-car one. In the steady-state case, the response to the harmonic excitation was analyzed, while in the transient one (Ahmadian and Vahdati, 2006), the response to the unit step. To ensure a compromise between the requirements for both comfort and safety, hybrid control with a MR damper is used (Goncalves and Ahmadian, 2003) and a combination of sky-hook and ground-hook control. The damping control algorithm was changed by a step function (on-off control) in order to simulate the behaviour of the damper between the constant reference point and a spring-supported (sky-hook – comfort) or non spring-supported mass (ground-hook – safety).

In the paper by Łuczko and Ferdek (2012), the effectiveness of damping of vibration of a quarter-car model by both semi-active and passive dampers was compared. Several different algorithms were proposed for semi-active dampers. The effect of these algorithms on the factors corresponding to driving safety and comfort were analyzed.

In this paper, analysis of a half-car model of a car by semi-active suspension is performed. The influence of parameters of the model on the efficiency of spring-supported mass damping is considered.

2. Half-car suspension model

Figure 1 shows the analyzed half-car model of an automobile. Vibration of the system around the static equilibrium position can be written using the following differential equations

$$\begin{aligned}
 m_{wf}\ddot{y}_{wf} &= -c_{wf}(\dot{y}_{wf} - \dot{w}_f) - k_{wf}(y_{wf} - w_f) + k_{bf}(y_{bf} - y_{wf}) - u_f \\
 m_{wr}\ddot{y}_{wr} &= -c_{wr}(\dot{y}_{wr} - \dot{w}_r) - k_{wr}(y_{wr} - w_r) + k_{br}(y_{br} - y_{wr}) - u_r \\
 m_b\ddot{y}_b &= -k_{bf}(y_{bf} - y_{wf}) - k_{br}(y_{br} - y_{wr}) + u_f + u_r \\
 I_b\ddot{\phi}_b &= l_f k_{bf}(y_{bf} - y_{wf}) - l_r k_{br}(y_{br} - y_{wr}) - l_f u_f + l_r u_r
 \end{aligned} \tag{2.1}$$

where y_{wf} and y_{wr} , are displacements of the front and rear suspension systems (i.e. the non-spring-supported mass m_{wf} and m_{wr}), y_{bf} and y_{br} are displacements of the points connecting the car body (spring-supported mass m_b of inertia I_b) with the suspension systems.

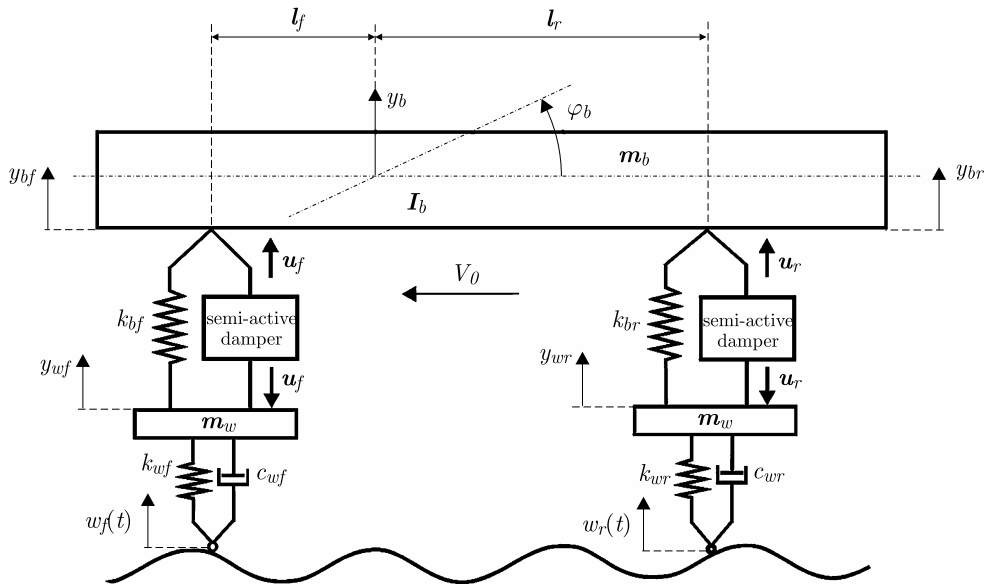


Fig. 1. Half-car model

Additionally, two parameters are introduced which are respectively: position y_b of the mass center and rotation angle ϕ_b of the car body. They can be found using the following equations (on the assumption of small displacements)

$$y_b = \frac{l_r y_{bf} + l_f y_{br}}{l} \quad \phi_b = \frac{y_{br} - y_{bf}}{l} \tag{2.2}$$

The function $w_f(t)$ and $w_r(t) = w_f(t - t_0)$ define the applied kinematic excitation, which corresponds to the profile of the road. The delay time t_0 is related to driving velocity V_0 and distance $l = l_f + l_r$ between both vehicle axles. The parameters: k_{wf} , k_{wr} and c_{wf} , c_{wr} define stiffness

and damping parameters of the front and rear wheel, while k_{bf} , k_{br} are stiffnesses of the front and rear spring respectively. The definition of forces u_f and u_r which are generated by semi-active dampers and applied to the non-spring-supported and spring-supported masses, are defined in Section 2 of this paper.

Equations (2.1) can be written in a matrix form. In order to do so, the third and the fourth equation of the system must be transformed (2.1), including additional relations (2.2). By choosing the displacements y_{wf} , y_{wr} , y_{bf} and y_{br} for coordinates of the vector \mathbf{y} , vibration of the system can be, after introduction of mass \mathbf{M} , damping \mathbf{C} and stiffness matrix \mathbf{K} , presented in form of the second-order matrix equation

$$\mathbf{M}\ddot{\mathbf{y}} + \mathbf{C}\dot{\mathbf{y}} + \mathbf{K}\mathbf{y} = \tilde{\mathbf{B}}\mathbf{u} + \tilde{\mathbf{F}}\mathbf{w}(t) \quad (2.3)$$

where $\mathbf{y} = [y_{wf}, y_{wr}, y_{bf}, y_{br}]^T$, $\mathbf{u} = [u_f, u_r]^T$ and $\mathbf{w} = [w_f, w_r]^T$. The stiffness matrix is as shown below

$$\mathbf{K} = \begin{bmatrix} k_{wf} + k_{bf} & 0 & -k_{bf} & 0 \\ 0 & k_{wr} + k_{br} & 0 & -k_{br} \\ -k_{bf} & 0 & k_{bf} & 0 \\ 0 & -k_{br} & 0 & k_{br} \end{bmatrix} \quad (2.4)$$

The damping matrix, after inclusion of passive dampers present in the vibroisolation systems, has the identical structure as the stiffness matrix. As damping properties of the wheels are usually omitted ($c_{wf} = c_{wr} = 0$) and the effect of passive dampers is already included in the forces u_f and u_r , the matrix \mathbf{C} is empty. The mass matrix can be presented in the form:

$$\mathbf{M} = \begin{bmatrix} \mathbf{M}_w & \mathbf{0} \\ \mathbf{0} & \mathbf{M}_b \end{bmatrix} \quad (2.5)$$

where

$$\mathbf{M}_w = \begin{bmatrix} m_{wf} & 0 \\ 0 & m_{wr} \end{bmatrix} \quad \mathbf{M}_b = \begin{bmatrix} \frac{m_b l_r^2 + I_b}{l^2} & \frac{m_b l_f l_r - I_b}{l^2} \\ \frac{m_b l_f l_r - I_b}{l^2} & \frac{m_b l_f^2 + I_b}{l^2} \end{bmatrix} \quad (2.6)$$

From Eqs (2.5) and (2.6), it can be seen that when the condition $m_b l_f l_r - I_b = 0$ is fulfilled, the matrix \mathbf{M} becomes diagonal, and with the matrix \mathbf{K} given in (2.4), decoupling of vertical vibration of the rear and front part of the vehicle, is possible. If the so-called ‘‘mass distribution index’’ $\lambda = I_b / m_b l_f l_r$ is close to 1, the excitation applied to one axle does not cause vibration of the other one. The matrices $\tilde{\mathbf{B}}$ and $\tilde{\mathbf{F}}$ can be written as follows

$$\tilde{\mathbf{B}} = \begin{bmatrix} -1 & 0 \\ 0 & -1 \\ 1 & 0 \\ 0 & 1 \end{bmatrix} \quad \tilde{\mathbf{F}} = \begin{bmatrix} k_{wf} & 0 \\ 0 & k_{wr} \\ 0 & 0 \\ 0 & 0 \end{bmatrix} \quad (2.7)$$

In order to transform matrix equation of motion (2.3) in the first-order form suitable for performing the numerical simulations, a modified state vector that includes velocities, is introduced

$$\mathbf{x} = \begin{bmatrix} \mathbf{x}_1 \\ \mathbf{x}_2 \end{bmatrix} = \begin{bmatrix} \mathbf{y} \\ \dot{\mathbf{y}} \end{bmatrix} \quad (2.8)$$

Motion of the system can be now written using the equation

$$\dot{\mathbf{x}} = \mathbf{A}\mathbf{x} + \mathbf{B}\mathbf{u} + \mathbf{F}\mathbf{w}(t) \quad (2.9)$$

The relation between the matrix A and the matrices present in equation (2.3) is

$$\mathbf{A} = \begin{bmatrix} \mathbf{0}^{(4 \times 4)} & \mathbf{I}^{(4 \times 4)} \\ -\mathbf{M}^{-1}\mathbf{K} & -\mathbf{M}^{-1}\mathbf{C} \end{bmatrix} \quad (2.10)$$

where $\mathbf{0}^{(4 \times 4)}$ and $\mathbf{I}^{(4 \times 4)}$ are, respectively, an empty and singular matrix of 4×4 size. The same holds for the matrices

$$\mathbf{B} = \begin{bmatrix} \mathbf{0}^{(4 \times 2)} \\ \mathbf{M}^{-1}\tilde{\mathbf{B}} \end{bmatrix} \quad \mathbf{F} = \begin{bmatrix} \mathbf{0}^{(4 \times 2)} \\ \mathbf{M}^{-1}\tilde{\mathbf{F}} \end{bmatrix} \quad (2.11)$$

where the matrix $\mathbf{0}^{(4 \times 2)}$ is an empty matrix of 4×2 size. Matrix equation (2.9) is well-suited for analysis of active systems in which the control vector \mathbf{u} is treated as the sought optimal control vector.

3. Semi-active dampers

The analysis presented below is limited to testing the effect of several selected half-car model parameters and two semi-active dampers on dynamical characteristics of the system. The forces generated by a simplified model of the semi-active damper (denoted as SA1) after introduction of the functions

$$u^{Lin}(\dot{y}_1, \dot{y}_2) = \begin{cases} c^{max}(\dot{y}_1 - \dot{y}_2) & \dot{y}_2(\dot{y}_1 - \dot{y}_2) \leq 0 \\ c^{min}(\dot{y}_1 - \dot{y}_2) & \dot{y}_2(\dot{y}_1 - \dot{y}_2) > 0 \end{cases} \quad (3.1)$$

can be calculated from the equations

$$\begin{aligned} u_f &= u^{Lin}(\dot{y}_{wf}, \dot{y}_{bf}) \\ u_r &= u^{Lin}(\dot{y}_{wr}, \dot{y}_{br}) \end{aligned} \quad (3.2)$$

In SA1 damper model, the forces are proportional to the relative velocity, with higher energy dissipation if the momentary power is less than zero (which means that energy is retrieved from the spring-supported mass). For $c^{max} = c^{min}$, equations (3.1) and (3.2) define the passive damper (PS).

The other type of a semi-active damper (SA2) is defined (Spencer *et al.*, 1996) using the Spencer model (Fig. 2). The mathematical description of the generated force is more complicated in this case. Based on the study by Ferdek and Łuczko (2011), a concise force definition can be presented

$$\begin{aligned} u_f &= u^{Spencer}(y_{wf}, \dot{y}_{wf}, \dot{y}_{bf}) \\ u_r &= u^{Spencer}(y_{wr}, \dot{y}_{wr}, \dot{y}_{br}) \end{aligned} \quad (3.3)$$

where

$$u^{Spencer}(y_1, \dot{y}_1, \dot{y}_2) = c_2(\dot{z}_1 - \dot{y}_2) \quad (3.4)$$

Additional parameters z_1 and z_2 can be obtained from the set of equations

$$\begin{aligned} k_1(y_1 - z_1) + c_1(\dot{y}_1 - \dot{z}_1) - \alpha_0 z_2 &= c_2(\dot{z}_1 - \dot{y}_2) \\ \dot{z}_2 &= A\dot{z}_0 \{1 - [\gamma + \beta \text{sgn}(z_2 \dot{z}_0)] |z_2|^n\} \end{aligned} \quad (3.5)$$

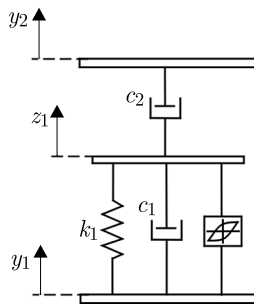


Fig. 2. Model of the semi-active Spencer damper

in which $z_0 = z_1 - y_1$ and $\beta + \gamma = 1$ ($0 < \beta < 1, 0 < \gamma < 1$). Equation (3.5)₁ can be interpreted as the equilibrium condition of forces acting on a massless middle element in the Spencer model (Fig. 2). The dimensionless variable z_2 , which is the solution of differential equation (3.5)₂ proposed in a similar form by Bouc-Wen (Spencer *et al.*, 1996), determined the appearance of a hysteresis. Its shape depends on the parameters A , γ , β and n . The parameters β and γ have impact on the characteristic only when A is small. In such a case, an increase in β causes the width of the hysteresis to be slightly decreased. Most often, when forming the characteristic, the value $n = 2$ is chosen, in rare cases $n = 1$ is taken. The parameter A is the one that strongly influences the shape of the hysteresis. With an increase in the parameter A , the lower and upper limits of the Bouc-Wen model characteristic are symmetrical. In the numerical calculations, emphasis is put on the analysis of coefficients α_0 , c_1 and c_2 and their impact on the solution. The parameters of $A = 50 \text{ m}^{-1}$, $\gamma = \beta = 0.5$ and $n = 2$ have been taken from the literature.

The slope of the force characteristic in the high velocity range depends on the value of a substitute damping coefficient $c_z = c_1 c_2 / (c_1 + c_2)$ with a relation close to linear. For lower velocities, the slope and inflection point of the characteristic are related to the parameter α_0 .

In the semi-active damper (e.g. magneto-rheological one), it is assumed that the parameters α_0 , c_1 and c_2 of the Spencer model are linearly dependent on the control voltage. By taking a control algorithm analogical to (3.1), it can be assumed that $c_k = p(\dot{y}_1, \dot{y}_2, c_k^{max}, c_k^{min})$, $k = 1, 2$ and $\alpha_0 = p(\dot{y}_1, \dot{y}_2, \alpha_0^{max}, \alpha_0^{min})$, with p defined using the formula

$$p(\dot{y}_1, \dot{y}_2, p^{max}, p^{min}) = \begin{cases} p^{max} & \dot{y}_2(\dot{y}_1 - \dot{y}_2) \leq 0 \\ p^{min} & \dot{y}_2(\dot{y}_1 - \dot{y}_2) > 0 \end{cases} \quad (3.6)$$

4. Results of numerical calculations

In the numerical calculations, the emphasis is placed on analyzing the effect of a few selected parameters of the system, with other parameters assumed as follows: $l_f = 0.94 \text{ m}$, $l_r = 1.66 \text{ m}$, $m_b = 510 \text{ kg}$, $m_{wf} = m_{wr} = 28 \text{ kg}$, $I_b = \lambda m_b l_f l_r$ (variable λ), $k_{wf} = k_{wr} = 180000 \text{ N/m}$, $k_b = 40000 \text{ N/m}$, $k_1 = 0.01 k_b$, $c_{wf} = c_{wr} = 0$, $A = 50 \text{ m}^{-1}$ and $\beta = \gamma = 0.5$. When analyzing the effect of stiffness of the front and rear suspension system, it is assumed that $k_{bf} = \kappa_k k_b$, $k_{br} = (1 - \kappa_k) k_b$, ($0 < \kappa_k < 1$), k_b – is the sum of stiffness parameters. Similarly, when considering the effect of energy dissipation, the parameters of PS damper are: $c_{bf} = \kappa_c c_b$, $c_{br} = (1 - \kappa_c) c_b$, ($0 < \kappa_c < 1$). The value of $c_b = 2260 \text{ Ns/m}$ has been chosen such that the dimensionless damping factor, given by equation

$$\zeta = \frac{c_b}{2m_b \omega_0} = \frac{c_{bf} + c_{br}}{2m_b \omega_0} \quad (4.1)$$

is $\zeta \approx 0.25$ – the recommended value for vehicle shock absorbers. The dimensionless angular velocity ω_0 (close to the two highest vibration modes of the system) present in Eq. (4.1) is defined as follows

$$\omega_0 = \sqrt{\frac{k_b}{m_b}} = \sqrt{\frac{k_{bf} + k_{br}}{m_b}} \quad (4.2)$$

When choosing the parameters of semi-active dampers, the same assumption is made regarding the parameters of front and rear dampers as well as the energy dissipation level. For SA1 damper, it is assumed that the mean value of damping coefficients are: $c_f^{mean} = \kappa_c c_b$, $c_r^{mean} = (1 - \kappa_c)c_b$, while the extreme values can be calculated from

$$p^{max} = (1 + \delta)p^{mean} \quad p^{min} = (1 - \delta)p^{mean} \quad (4.3)$$

where $p = c_f$ or $p = c_r$ and $0 < \delta < 1$.

SA2 damper has a higher number of significant parameters. Formulas (4.3) need to be used for the extreme parameters α_0 , c_1 and c_2 of the front and rear damper, while the mean values c_{1f}^{mean} , c_{2f}^{mean} , c_{1r}^{mean} and c_{2r}^{mean} must be chosen such that the coefficient ζ has the desired value. From literature (Prabakar *et al.*, 2009; Spencer *et al.*, 1996), it can be seen that c_{1f}^{mean} , c_{1r}^{mean} values are an order lower from c_{2f}^{mean} , c_{2r}^{mean} ones. These are chosen as follows: $c_{1f} = 1.1\kappa_c c_b$, $c_{2f} = 11\kappa_c c_b$, $c_{1r} = 1.1(1 - \kappa_c)c_b$ and $c_{2r} = 11(1 - \kappa_c)c_b$. For the chosen values, the relation $c_{zf} + c_{zr} = c_b$, where $c_z = c_1 c_2 / (c_1 + c_2)$ is true and coefficient (4.1) is equal to $\zeta = 0.25$.

The values of varying parameters are presented with analysis of the results of numerical simulations. When presenting the results, the dimensionless parameters are introduced relating the displacements with the excitation amplitude a_0 , velocities with the value $\omega_0 a_0$, while accelerations with $\omega_0^2 a_0$, and forces with $k_b a_0$.

One of less known parameters of the system is the delay time t_0 between the functions describing motion of the front and rear wheel of the vehicle. In order to estimate it, it is assumed that the angular frequency of the kinematic excitation ω is related for the given road profile linearly with the velocity V_0 , or using the formula: $\omega = \mu V_0$. For motion with constant velocity V_0 , the relation $t_0 = l/V_0$, where l is the distance between both axles, is also true. By additionally assuming that the lowest vibration mode of the approximate frequency ω_0 is related to a known velocity V_r , the value of the parameter $\mu = \omega_0/V_r$ and the delay time $t_0 = \omega_0 l/V_r \omega$ can be calculated, e.g. for given: $V_r = 20$ km/h, $l = 2.6$ m and $\omega_0 = 8.856$ rd/s a value of $t_0 \approx 4.15/\omega$ is found.

The frequency characteristics are ideal for the purpose of global evaluation of dynamical properties of the system. In the simulations, the kinematic excitation is usually defined by the harmonic function of a modulated angular frequency: (e.g. “Chirp Signal” in Simulink). If the simulation time is high enough, an approximate frequency characteristic can be acquired by graphing the maximal responses of the system.

In order to illustrate the effect of car body mass distribution, characteristics of maximal dimensionless velocities $v_{bf} = \dot{x}_3/\omega_0 a_0$ and $v_{br} = \dot{x}_4/\omega_0 a_0$ (in the points connecting the body and the suspension) with relation to the dimensionless angular frequency of the excitation $\eta = \omega/\omega_0$ are shown in Fig. 3. The analysis is limited to vibration comparison of systems with identical shock absorbers ($\kappa_k = \kappa_c = 0.5$). The parameter defining the semi-active damper has been chosen as $\delta = 0.5$. The only modified value is the mass distribution ratio λ . The corresponding inertia of the spring-supported mass is $I_b = \lambda m_b l_f l_r \approx 795.8\lambda$. The actual value of λ should be close to one. Several exemplary values of this coefficient, calculated from the data presented in the literature, are equal: $\lambda = 1.01$ (Feng *et al.*, 2003), $\lambda = 1.09$ (Sam *et al.*, 2008), $\lambda = 1.16$ (Lozia *et al.*, 2008), $\lambda = 0.823$ (Prabakar *et al.*, 2009). However, in some cases this value is different, e.g. (Shamsi and Choupani, 2008) $\lambda = 0.544$, which is far from one.

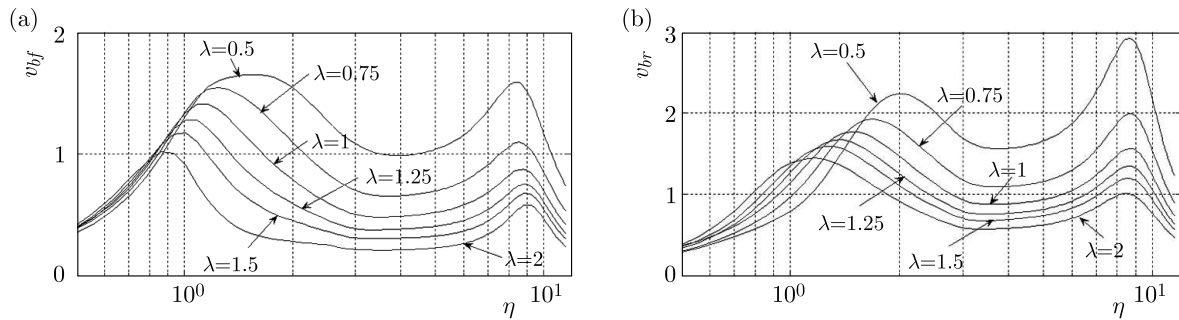


Fig. 3. Effect of spring-supported mass distribution on the frequency characteristics: (a) velocity v_{bf} , (b) velocity v_{br}

From the results presented in Fig. 3, it can be seen that the lower the coefficient λ becomes, the larger are the maximal velocities, especially within the resonance regimes. Although this model has four degrees of freedom, only two resonance regions can be seen on the presented frequency characteristics. This is caused by close proximity of the paired natural frequencies of the system. For example, when $\lambda = 0.5$, the natural frequency values of the linearized system related to ω_0 are equal to: 0.88 (dominant displacement of the front part of the vehicle), 1.44 (rear part), 8.97 and 9.16 (wheel vibration), while for $\lambda = 2$ these values are respectively: 0.67, 0.97, 9.14 and 9.21.

A consequence of such a distribution of frequencies is dislocation of the lowest frequency region towards the lower frequency with an increase in λ and its slightly different disposition in the velocity characteristics v_{bf} and v_{br} . The location of the “second” region is less vulnerable to a change in the parameter λ and is similar to Fig. 3a and Fig. 3b.

Although the obtained results are only for SA1 damping system, the conclusions are more general, and essentially similar results are obtained for PS and SA2 systems.

In the case of SA2 system described by the Spencer model, the effectiveness of the damper, depends on chosen values of c_{1f}^{mean} , c_{2f}^{mean} , c_{1r}^{mean} , c_{2r}^{mean} and δ , but mostly on the parameter α_0 . Fig. 4 shows the dimensionless displacement characteristics $x_{wf} = x_1/a_0$ (non-spring-supported mass) and $x_{bf} = x_3/a_0$ (spring-supported mass) for several values of the parameter $\alpha = \alpha_0^{mean}/\alpha_0^{mean}k_b a_0$. At $\kappa_c = 0.5$ (symmetrical support), the relations are: $c_{1f} = c_{1r} = 0.55c_b$, $c_{2f} = c_{2r} = 5.5c_b$ and the mean value of the coefficient ζ is close to 0.25. By analyzing Fig. 4b, one can see that the characteristic closest to the optimal is the curve obtained for $\alpha = 0.5$. Too high values of α cause the forces to be much higher for low velocities, and also shift the inflation point location, which is undesirable especially in the range of high-frequency excitation. From the graphs shown in Fig. 4a, it can be concluded that within the range of high oscillation, which includes the third and fourth natural frequencies, the amplitudes of non-spring-supported

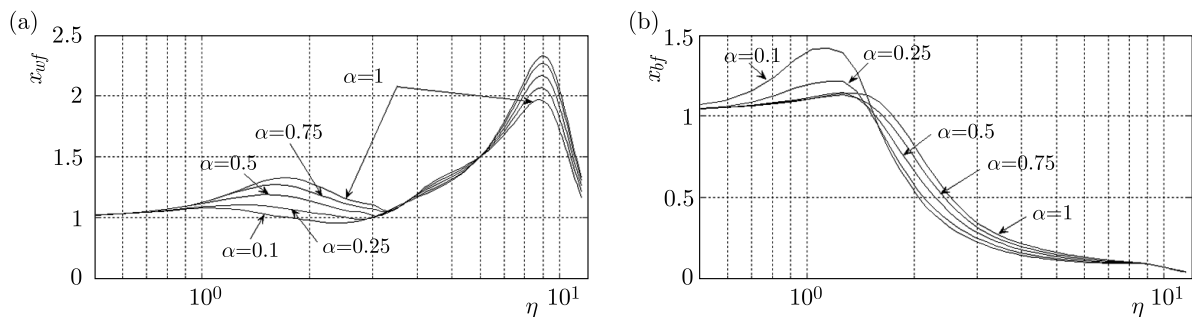


Fig. 4. Effect of the parameter α on the frequency characteristics of SA2 system: (a) displacement x_{wf} , (b) displacement x_{bf}

masses (wheels) are significant. Additionally, within this range, the dynamic response values are also large, and so the indexes related to the driving safety and comfort are lower, which means that these semi-active dampers are not efficient.

In order to compare SA1 and SA2 dampers, the dimensionless force characteristics $U_f = u_f/k_b a_0$ generated by both types of semi-active dampers are shown in Fig. 5. Only the front part of the car suspension is presented. As before, it is assumed that $\kappa_k = \kappa_c = 0.5$, (symmetrical model) with $\lambda = 1$, $\alpha = 0.5$, $\zeta = 0.25$ and $\delta = 0.5$.

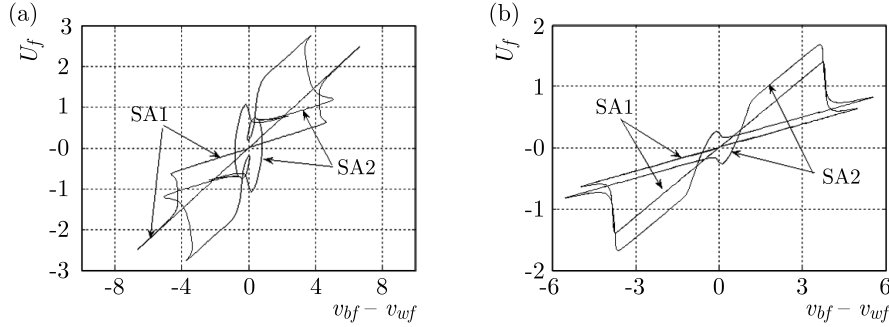


Fig. 5. Damper SA1 and SA2 characteristics: (a) $\omega = 1$, (b) $\omega = 4$

The characteristic of SA1 damper is relatively simple. Two of its branches are straight lines of slopes equal to the given c_f^{min} and c_f^{max} values, while the lines linking the other two, should be, in theory, vertical. The reason for this deviation is due to the approximation used for the continuous switching step function (based on arctan). Such an approach is recommended for discontinuous functions due to its accuracy and the time of numerical computation required, and also in some cases for avoidance of undesirable effects caused by too frequent switching, e.g. chattering.

The characteristic of SA2 damper in the range of high velocities is similar to the one described above. The differences are visible within the range of low velocities. The average slope of the characteristic is higher and depends primarily on the parameter α . The higher complexity of the graph is also due to the other parameters of the half-car model. Less complex characteristics can be obtained by analyzing a simpler model, such as a quarter-car model (Łuczko and Ferdek, 2012).

Figure 6 shows the frequency response of dimensionless displacements $x_{bf} = x_3/a_0$ and $x_{br} = x_4/a_0$ for passive PS and both semi-active SA1 and SA2 systems.

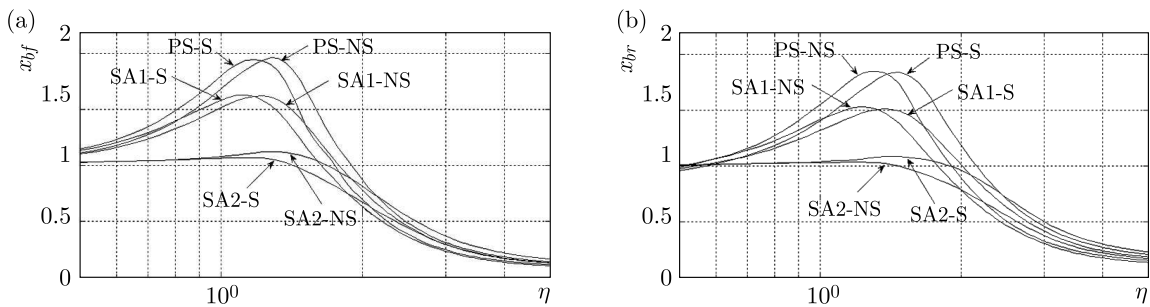


Fig. 6. Effect of the parameters κ_k and κ_c on frequency characteristics PS, SA1 and SA2:
(a) displacement x_{bf} , (b) displacement x_{br}

The case of symmetrical mounting $\kappa_k = \kappa_c = 0.5$ (S systems, Fig. 6) and the asymmetrical one defined by parameters: $\kappa_k = \kappa_c = l_r/l_f \approx 0.638$ (NS systems) is considered. For selected values of the parameter κ_k , the static deflections of the spring-supported mass under its own mass are identical in both locations of the connection with the suspension systems, while the

center of stiffness overlaps the center of mass. The values $\lambda = 1$, $\alpha = 0.5$, $\zeta = 0.25$ and $\delta = 0.5$ have been assumed, while the other parameters of the Spencer model have been obtained using appropriate equations with known parameters κ_k and κ_c . When showing the results, only the region with the lowest natural mode (actually two lowest modes) are shown – the ones in which the car body vibration is dominant.

As the parameters for models PS, SA1 and SA2 are chosen in such a way that the natural frequencies are the same for the identical parameter κ_k , the dislocation of the resonance region is avoided. Such a dislocation is only visible between the curves obtained for $\kappa_k = 0.5$ (S systems) and $\kappa_k = 0.638$ (NS systems). The value of the parameter κ_k influences mostly the two lowest natural frequencies. The complex natural frequencies (related to ω_0) are equal: $\eta_1 = -0.16 \pm 0.83i$, $\eta_2 = -0.29 \pm 1.10i$ for S systems and: $\eta_1 = -0.195 \pm 0.927i$, $\eta_2 = -0.217 \pm 0.945i$ for NS ones.

The location of the resonance regions, as shown in Figs. 6a and 6b is directly related to the distribution of the natural frequencies of S and NS systems. As the low values correspond to the natural modes in which the displacement are dominant (and even more x_{br}), the resonance frequency of S systems is lower than that in NS ones for characteristics of the displacement x_{bf} (Fig. 6a). The opposite effect is observed for the displacement x_{br} (Fig. 6b).

The vibration reduction level is indeed related to the parameter κ_k (at least within the analyzed regimes). Using a more stiff front mounting, the comfort of the driver is only slightly decreased but seems to be important when considering safety of the driver (this is not a subject of analysis in this study). The systems with SA1 dampers reduce vibration by around 20% when compared with passive ones, while the semi-active SA2 dampers are proved to be even more effective, reducing the values of the displacement x_{bf} and x_{br} twice in the fundamental resonance.

Figure 7 shows the response of PS, SA1 and SA2 dampers (dimensionless displacements x_{bf} and x_{br} , velocities v_{bf} and accelerations a_{bf} in function of the dimensionless time $\tau = \omega_0 t$) to an impulse excitation defined by equation (Shekhar *et al.*, 1999; Łuczko, 2011)

$$w_f(t) = \frac{e}{4} a_0 \sum_{k=1}^3 \omega_k (t - t_k)^2 \exp[-\omega_k (t - t_k)] H(t - t_k) \quad (4.4)$$

where $H()$ is the unit step function. Function (4.4) is supposed to simulate the vehicle crossing the same obstacle at three different velocities $V_0 = \theta V_r$ (where $\theta = 1/2, 1, 4$), which in equations (4.4) are represented by angular frequencies $\omega_1 = 0.5\omega_0$, $\omega_2 = \omega_0$ and $\omega_3 = 4\omega_0$. The values of t_k

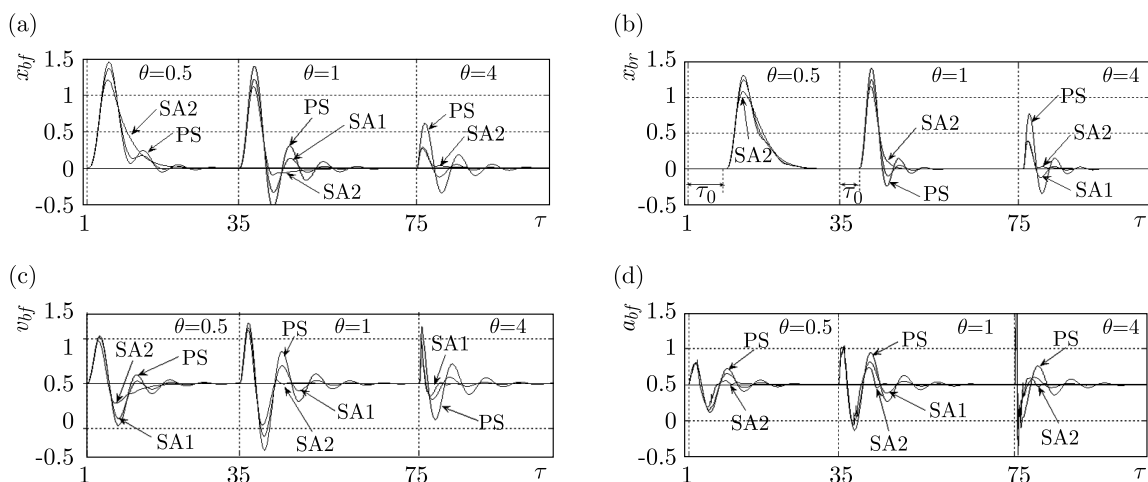


Fig. 7. Response of the system to an impulse excitation: (a) x_{bf} , (b) x_{br} , (c) v_{bf} , (d) a_{bf}

are chosen in such a way that the vibration caused by the previous impulse would vanish before the next one is applied.

When crossing the obstacle at a low speed ($\theta = 0.5$ and $\theta = 1$), the maximum displacements (Fig. 7a and Fig. 7b) are to a small extent related with the type of a damper, although the lowest ones are obtained for SA2 damper. The type of the used damper has a greater effect on the character of damping of vibration caused by an impulse excitation. For PS and SA1 systems, reduction of oscillatory vibration can be observed. In the case of SA2 systems, the damping is much faster and similar in shape to an exponential function. For high values of velocity, when crossing the obstacle ($\theta = 4$), the displacements are definitely lower. This is however at the cost of large acceleration values (Fig. 7d), for which the maximum values are practically independent of the type of the used vibroisolation system. With an increase in driving velocity, the time delay t_0 is decreased while the displacements of both front and back parts of the body are similar.

5. Summary

Based on the analysis of selected results of numerical calculations, several conclusions can be drawn:

- The algorithms for control of a semi-active on-off damper in which the switching is related to the actual power, enable improvement the driving comfort, especially within the low-frequency excitation range.
- From the tested dampers, definitely the best one is SA2 damper with a nonlinear characteristic. If the parameters for the damper are optimal, the vibration amplitude can be reduced twice as much within the range of fundamental resonance.
- Semi-active SA2 system is also effective when subjected to an impulse excitation which simulates obstacles (bumps) in the road.
- An improper mass distribution (low values of λ) might be an additional cause for an increased vibration level of the spring-supported mass.
- The introduction of an additional spring and damping elements to the front and back car suspension in which the center of stiffness overlaps the center of mass, does not cause a decrease in the indexes describing the driving comfort. It might be, however, beneficial when considering the safety.
- Semi-active systems are less efficient than passive ones when the driving velocity (excitation frequency) is high.

References

1. AHMADIAN M., 2001, Active control of vehicle vibrations, *Encyclopedia of Vibration*, Academic Press, London, 37-48
2. AHMADIAN M., VAHDATI N., 2006, Transient dynamics of semiactive suspensions with hybrid control, *Journal of Intelligent Material Systems and Structures*, **17**, 2, 145-153
3. CROSBY M.J., KARNOPP D.C., 1973, The active damper – a new concept for shock and vibration control, *Shock and Vibration Bulletin*, **43**, 119-133
4. DOMINGUEZ A., SEDAGHATI R., STIHARU I., 2008, Modeling and application of MR dampers in semi-adaptive structures, *Computers and Structures*, **86**, 407-415
5. FENG J.Z., LI J., YU F., 2003, GA-based PID and fuzzy logic control for active vehicle suspension system, *International Journal of Automotive Technology*, **4**, 4, 181-191

6. FERDEK U., ŁUCZKO J., 2011, Analysis of the quarter-car model suspension of a vehicle with a hydraulic damper (in Polish), *Symulacja w Badaniach i Rozwoju*, **2**, 2, 67-74
7. FISCHER D., ISERMANN R., 2004, Mechatronic semi-active and active vehicle suspensions, *Control Engineering Practice*, **12**, 1353-1367
8. GONCALVES F.D., AHMADIAN M., 2003, A hybrid control policy for semi-active vehicle suspensions, *Shock and Vibration*, **10**, 1, 59-69
9. GOPALA RAO L.V.V., NARAYANAN S., 2009, Sky-hook control of nonlinear quarter car model traversing rough road matching performance of LQR control, *Journal of Sound and Vibration*, **323**, 515-529
10. HUANG S-J, CHEN H-Y., 2006, Adaptive sliding controller with self-tuning fuzzy compensation for vehicle suspension control, *Mechatronics*, **16**, 607-622
11. IHSAN S., AHMADIAN M., FARIS W., BLANCHARD E.D., 2009, Ride performance analysis of half-car model for semi-active system using RMS as performance criteria, *Shock and Vibration*, **16**, 6, 593-605
12. LIU Y., WATERS T.P., BRENNAN M.J., 2005, A comparison of semi-active damping control strategies for vibration isolation of harmonic disturbances, *Journal of Sound and Vibration*, **280**, 21-39
13. LOZIA Z., SIMIŃSKI P., ZDANOWICZ P., 2008, The effect of the position of the center of mass on behaviour of the LTV vehicle in curvilinear motion (in Polish), *Czasopismo Techniczne*, 6-M, 65-83
14. ŁUCZKO J., 2011, Comparison of dynamical responses of semi-active dampers described by the Bouc-Wen and Spencer models (in Polish), *Czasopismo Techniczne*, **2**, 1-M, 127-136
15. ŁUCZKO J., FERDEK U., 2012, Comparison of different control strategies in a semi-active vehicle suspension system (in Polish), *Czasopismo Techniczne*, **11**, 6-M, 81-92
16. PRABAKAR R.S., SUJATHA C., NARAYANAN S., 2009, Optimal semi-active preview control response of a half car vehicle model with magnetorheological damper, *Journal of Sound and Vibration*, **326**, 400-420
17. SAM Y.M., SUAIB N.M., OSMAN J.H.S., 2008, Hydraulically actuated active suspension system with proportional integral sliding mode control, *WSEAS Transactions on Systems and Control*, **9**, 3, 859-868
18. SAPIŃSKI B., MARTYNOWICZ P., 2005, Vibration control in a pitch-plane suspension model with MR shock absorbers, *Journal of Theoretical and Applied Mechanics*, **43**, 3, 655-674
19. SAPIŃSKI B., ROSÓŁ M., 2008, Autonomous control system for a 3DOF pitch-plane suspension model with MR shock absorbers, *Computers and Structures*, **86**, 379-385
20. SHAMSI A., CHOUPANI N., 2008, Continuous and discontinuous shock absorber, Control through skyhook strategy in semi-active suspension system (4DOF Model), *International Journal of Mechanical, Industrial and Aerospace Engineering*, 254-258
21. SHEKHAR N.C., HATWAL H., MALLIK A.K., 1999, Performance of non-linear isolators and absorbers to shock excitations, *Journal of Sound and Vibration*, **227**, 2, 293-307
22. SPENCER JR B.F., DYKE S.J., SAIN M.K., CARLSON J.D., 1996, Phenomenological model for magnetorheological dampers, *ASCE Journal of Engineering Mechanics*, **123**, 3, 230-238
23. WU X., GRIFFIN M.J., 1997, A semi-active control policy to reduce the occurrence and severity of end-stop impacts in a suspension seat with an electrorheological fluid damper, *Journal of Sound and Vibration*, **203**, 5, 781-793
24. YAO G.Z., YAP F.F., CHEN G., LI W.H., YEO S.H., 2002, MR damper and its application for semi-active control of vehicle suspension system, *Mechatronics*, **12**, 963-973